Tutorial on Input Shaping/Time Delay Control of Maneuvering Flexible Structures

Tarunraj Singh
Dept. of Mech. & Aero. Eng.,
University of Buffalo,
Buffalo, NY 14260
tsingh@eng.buffalo.edu
http://code.eng.buffalo.edu/tdf/

William Singhose
Dept. of Mech. Eng.,
Georgia Institute of Technology
Atlanta, Georgia, 30332
Bill.Singhose@me.gatech.edu
http://www.me.gatech.edu/inputshaping/

Abstract

Precise position control and rapid rest-to-rest motion is the desired objective in a variety of applications. The desire for reducing the maneuver time requires reducing the inertia of the structure which subsequently results in low frequency dynamics. The requirement of precise position control implies that the residual vibration of the structure should be zero or near zero. This paper presents techniques to shape the input to the system so as to minimize the residual vibration. A second class of problems which includes design of input profiles for systems with rigid-body modes driven by actuators with finite control authority, is also presented. The common thread which connects all the techniques presented in this paper is related to the design of controllers which are robust to modeling uncertainties. The proposed techniques are illustrated by simulations and experiments.

1 Introduction

Smith [1], Calvert and Gimple [2] proposed a simple technique to generate non-oscillatory response from an lightly-damped system subject to a step input. This is achieved by exciting two transient oscillations so as to result in constructive cancellation of the oscillations. Smith termed the technique *Posicast* motivated by what he states: " This is what happens when a fisherman drops his fly in the water at the maximum-position and zero velocity instant" [1]. Tallman and Smith [3] illustrated the Posicast technique using an analog computer and noted the sensitivity of the controller to

variation in the location of the poles of the system caused by nonlinear components in the system or variation of the parameters of the system as a function of temperature.

Between the late 50's and the publication of the *Input Shaping* paper by Singer and Seering [8], there was some work on the shaping of input profiles for control of residual vibration [4], [5]. Swigert [5] proposed techniques for the determination of torque profiles which considered the sensitivity of the terminal states to variations in the model parameters. Publication of the *Input Shaping* paper renewed interest in prefiltering reference inputs for robust vibration control, which has resulted in dozens of papers with application to spacecrafts, robots, cranes, chemical processes, etc. A chronological listing of papers relevant to robust vibration control of slewing structures is presented in the bibliography.

This paper will consider two classes of problems: The first, involves real-time shaping or time-delay filtering of the reference command to stable systems with the objective of minimizing the residual vibration [1] [8], [16], [23]. This will be dealt in detail in Section 2. The second class of problems considered is the design of controllers for systems with rigid body modes with constraints on the control input [7], [9], [14], [29], [49]. This can be further classified into two categories which will be expounded in Section 3. Sections 2 and 3 will describe in detail, technique for reducing the sensitivity of the control profile to errors in model parameters such as damping ratio, and natural frequency. Section 4 will briefly address the design of robust controllers for nonlinear systems [41].

Finally, Section 5 will describe some applications where the proposed techniques have been successfully implemented.
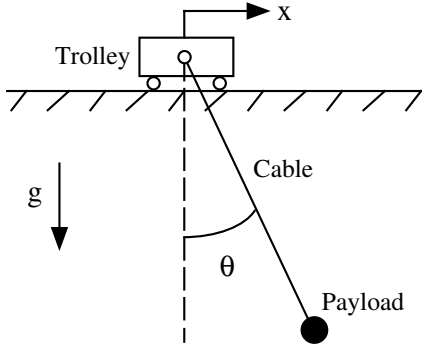
2 Real Time Command Shaping


Figure 1: Overhead Gantry Crane

There are all types of possible solutions to the problem of flexible dynamics including feedback control, feedforward control, command shaping, and even redesigning the physical hardware. A simple example of this challenging area is presented by an overhead gantry crane like the one shown schematically in Figure 1 . The payload is hoisted up by a cable. The upper end of the cable is attached to a trolley which travels along a rail to position the payload.

Cranes are controlled by a human operator who moves levers or presses buttons to cause the trolley to move. If the operator simply presses the control button for a finite time period, then the trolley will move a finite distance and come to rest. The payload on the other hand, will usually oscillate about the new trolley position. The payload position for a typical trolley movement is shown in Figure 2a.

An experienced crane operator can sometimes produce the desired payload motion with a small amount of residual vibration by pressing the button multiple times at the proper instances. The payload position for such a situation is shown in Figure 2b.

2.1 Simple Zero Vibration Command
As a first step to understanding how to generate commands that move systems without vibration,
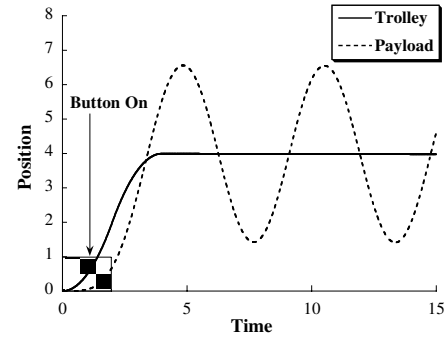
(a)
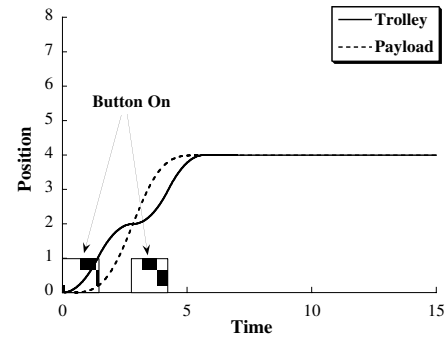
(b)

Figure 2: Crane Response: a) Unshaped Command b) Shaped Command

it is helpful to start with the simplest such command. We know that giving the system an impulse will cause it to vibrate; however, if we apply a second impulse to the system, we can cancel the vibration induced by the first impulse. This concept is shown in Figure 3.

At this point, it is useful to derive the amplitudes and time locations of the two-impulse command shown in Figure 3. If we have a reasonable estimate of the system's natural frequency, ω, and damping ratio, ζ, then the residual vibration that results from a sequence of impulses can be described by:

$$V(\omega, \zeta) = e^{-\zeta \omega t_n} \sqrt{C(\omega, \zeta)^2 + S(\omega, \zeta)^2} \qquad (1)$$

where,

$$C(\omega, \zeta) = \sum_{i=1}^{n} A_i e^{\zeta \omega t_i} cos(\omega_d t_i),$$

$$S(\omega, \zeta) = \sum_{i=1}^{n} A_i e^{\zeta \omega t_i} sin(\omega_d t_i) \qquad (2)$$
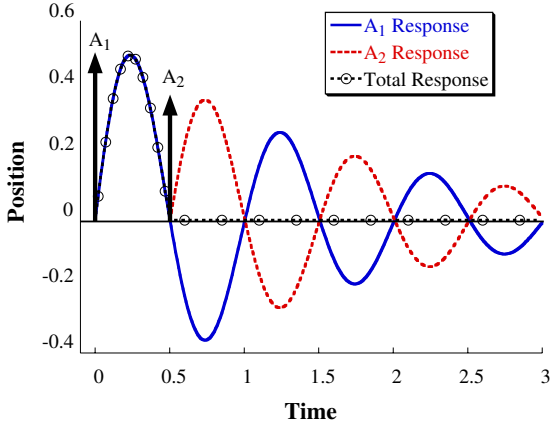
Figure 3: Two Impulse Response

A_i and t_i are the amplitudes and time locations of the impulses, n is the number of impulses in the impulse sequence, and $\omega_d = \omega\sqrt{1-\zeta^2}$. Equation 1 is actually the percentage residual vibration. It tells us how much vibration a sequence of impulses will cause, relative to the vibration caused by a single, unity-magnitude impulse. By setting (1) equal to zero, we can solve for the impulse amplitudes and time locations that would lead to zero residual vibration. However, we must place a few more restrictions on the impulses, or the solution will converge to zero-valued or infinitely-valued impulses. To avoid the trivial solution of all zero-valued impulses and to obtain a normalized result, we require the impulses to sum to one:

$$\sum A_i = 1. \tag{3}$$

Impulses could satisfy (3) by taking on very large positive and negative values. One way to obtain a bounded solution is to limit the impulse amplitudes to finite values or to positive values:

$$A_i > 0, \ i = 1,2,....,n \tag{4}$$

The problem we want to solve can now be stated explicitly: find a sequence of impulses that makes (1) equal to zero, while also satisfying (3) and (4). For a two-impulse sequence, the problem has four unknowns - the two impulse amplitudes (A_1, A_2) and the two impulse time locations (t_1, t_2). Without loss of generality, we can set the time location of the first impulse equal to zero, $t_1 = 0$. The problem is now reduced to finding three unknowns (A_1, A_2, t_2). In order for (1) to equal zero, the expressions in (2) must both equal zero independently

because they are squared in (1). Therefore, the impulses must satisfy:

$$0 = A_1 + A_2 e^{\zeta\omega t_2}cos(\omega_d t_2) \tag{5}$$

$$0 = A_2 e^{\zeta\omega t_2}sin(\omega_d t_2) \tag{6}$$

Equation (6) can be satisfied in a nontrivial manner, when the sine term equals zero. This occurs when:

$$\omega_d t_2 = n\pi, \Rightarrow t_2 = \frac{n\pi}{\omega_d} = \frac{nT_d}{2} \ \text{n=1,2,..} \tag{7}$$

where T_d is the damped period of vibration. This result tells us that there is an infinite number of possible values for the location of the second impulse - they occur at multiples of the half period of vibration. To cancel the vibration in the shortest amount of time, choose the smallest value for t_2:

$$t_2 = \frac{T_d}{2} \tag{8}$$

For this simple case, the amplitude constraint given in (3) reduces to:

$$A_1 + A_2 = 1 \tag{9}$$

Using the expression for the damped natural frequency and substituting (8) and (9) into (5) gives:

$$0 = A_1 - (1 - A_1)exp(\frac{\zeta\pi}{\sqrt{1-\zeta^2}}) \tag{10}$$

Rearranging (10) and solving for A_1 gives:

$$A_1 = \frac{exp(\frac{\zeta\pi}{\sqrt{1-\zeta^2}})}{1 + exp(\frac{\zeta\pi}{\sqrt{1-\zeta^2}})} \tag{11}$$

Defining $K = exp(\frac{-\zeta\pi}{\sqrt{1-\zeta^2}})$, the sequence of two impulses that leads to zero residual vibration can now be summarized as:

$$\begin{bmatrix} A_i \\ t_i \end{bmatrix} = \begin{bmatrix} \frac{1}{1+K} & \frac{K}{1+K} \\ 0 & 0.5T_d \end{bmatrix} \tag{12}$$

2.2 Using Zero-Vibration Impulse Sequences to Generate Zero-Vibration Commands

Real systems cannot be moved around with impulses, so we need to convert the properties of the impulse sequence given in (12) into a usable command. This can be done in a very simple way.
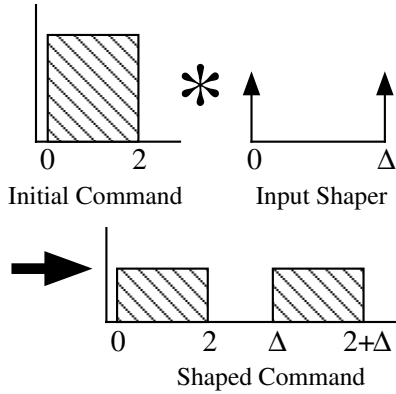
Figure 4: Multi Pulse Shaped Input

The impulse sequence is convolved with any desired command signal. The convolution product is then used as the command to the system. If the impulse sequence causes no vibration, then the convolution product will also cause no vibration.

This command generation process, called input shaping, is demonstrated in Figure 4 for an initial command that is a pulse function and a two-impulse input shaper. Note that the convolution product in this case is the two-pulse command similar to that shown in Figure 2b. But in most cases the impulse sequence will be much shorter than the command profile. When this occurs, the components of the shaped command that arise from the individual impulses run together as shown in Figure 5.
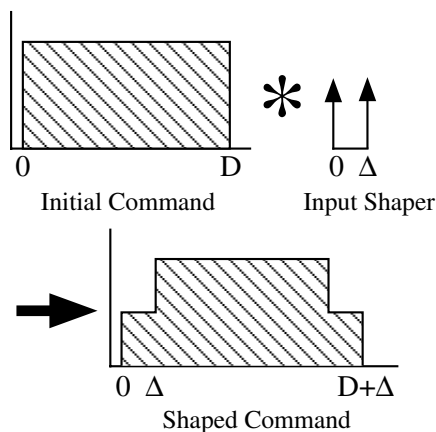

Figure 5: Continuous Shaped Input

2.3 Robustness to Modeling Errors
The amplitudes and time locations of the impulses depend on the system parameters (ω and ζ). If there are errors in these values (and there always are), then the impulse sequence will not result in zero vibration. In fact, for the two-impulse sequence discussed above, there can be a lot of vibration for a small modeling error. This lack of robustness was a major stumbling block for the original formulation that was developed in the 1950's. This problem can be visualized by plotting a sensitivity curve that shows the amplitude of residual vibration as a function of the system parameters. One such sensitivity curve for the zero-vibration (ZV) shaper is shown in Figure 6 with the normalized frequency on the horizontal axis and the percentage vibration on the vertical axis. Note that as the actual frequency deviates from the modeling frequency, the amount of vibration increases rapidly. The robustness can be measured quantitatively by measuring the width of the curve at some low level of vibration. This non-dimensional robustness measure is called the shaper's insensitivity. The 5% insensitivity has been labeled in Figure 6.
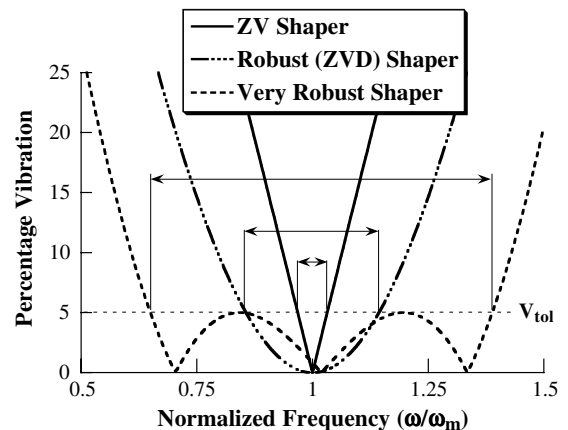

Figure 6: Sensitivity Curves

In order to increase the robustness of the input shaping process, the shaper must satisfy additional constraints. One such constraint sets the derivative of (1), with respect to frequency, equal to zero [8]. That is:

$$0 = \frac{d}{d\omega} V(\omega, \zeta) \qquad (13)$$

When this additional constraint is satisfied with V = 0, the result is a Zero Vibration and Derivative (ZVD) shaper [8]. By comparing the 5% insensitivities shown in Figure 6, it can be concluded
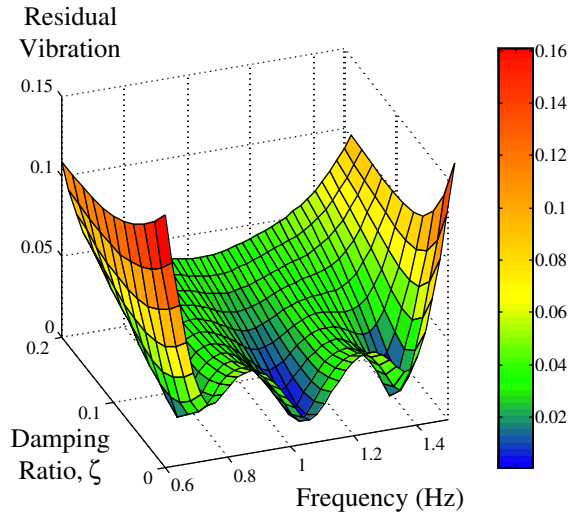
Figure 7: Three Dimensional Curve

Figure 8: Specified-Insensitivity Shaper

that the ZVD shaper is significantly more robust to modeling errors than the ZV shaper.

Since the development of the ZVD shaper, several other robust shapers have been developed. In fact, shapers can now be designed to have any amount of robustness to modeling errors [38]. The sensitivity curve for a very robust shaper is shown in Figure 6. Robustness is not restricted to errors in the frequency. Figure 7 shows a three-dimensional sensitivity curve for a shaper that was designed to suppress vibration between 0.7 Hz and 1.3 Hz and also over the range of damping ratios between 0 and 0.2. The shapers corresponding to these curves were designed using the Specified-Insensitivity (SI) approach. The most straightforward method for generating a shaper with specified insensitivity to modeling errors is the technique of frequency sampling [19], [38]. This method requires repeated use of the vibration amplitude equation, (1). In each case, V(ω,ζ) is set less than or equal to a tolerable level of vibration, V_{tol}:

$$V_{tol} > e^{-\zeta \omega_s t_n} \sqrt{C(\omega_s, \zeta)^2 + S(\omega_s, \zeta)^2}, \ s = 1,..., m \tag{14}$$

where ω_s represents the m unique frequencies at which the vibration is limited.

For example, if the shaper needs to suppress vibration for frequency errors of 20%, then the constraint equations limit the vibration to below V_{tol} at specific frequencies between $0.8\omega_n$ and $1.2\omega_n$. This procedure is illustrated in Figure 8 for V_{tol}
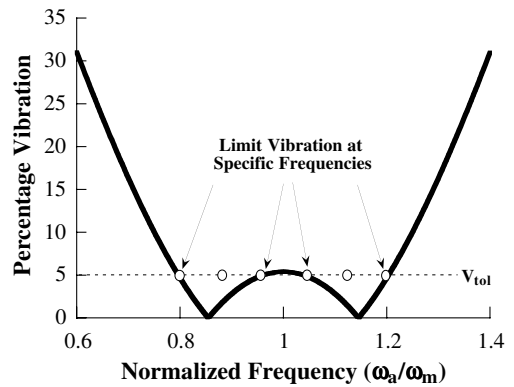
= 5%. Another technique related to SI shaping minimizes the expected level of residual vibration over a specified frequency range [52]. This technique has the advantage of taking into account any known distribution of the frequencies in the range being suppressed.

Any shaped command will have its rise time increased by the duration of the shaper as is shown in Figure 9a. Because the duration of the ZVD shaper is twice that of the ZV shaper, the ZVD shaper increases the rise time more than the ZV shaper. This increased rise time is the price that is paid for the increased robustness to modeling errors. With the SI shapers, increasing robustness increases rise time in a nonlinear manner. This leads to certain operating points that are advantageous [3].

For example, the ZVD shaper has a duration of only 1 period of the natural frequency. This time penalty is a small price to pay for the excellent robustness to modeling errors. To demonstrate this tradeoff, Figure 9 shows the response of a spring-mass system to step commands shaped with the three shapers shown in Figure 6. Figure 9a shows the response when the model is perfect and Figure 9b shows the case when there is a 30% error in the frequency estimate. The increase in rise time caused by the shapers is apparent in Figure 9a, while Figure 9b shows the vast improvement in vibration reduction that the robust shapers provide in the presence of modeling errors.

The techniques mentioned above produce robustness built into the design of the input shaper. There are other approaches to achieve robust in-
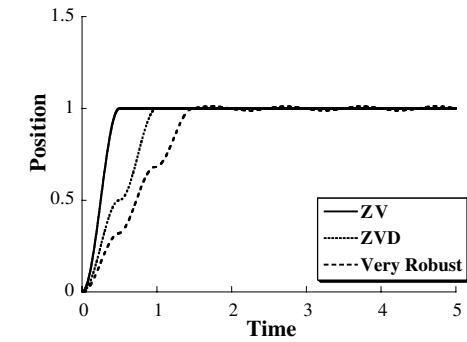
(a)
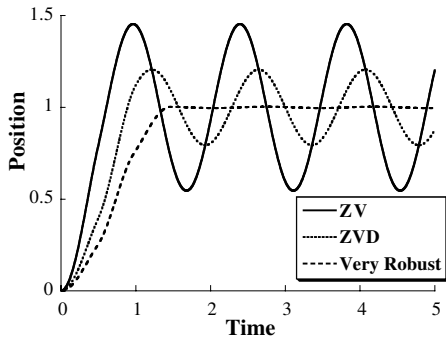
(b)

Figure 9: System Response: a) Perfect Knowledge, b) 30% Error

put shaping. Several researchers have used adaptive input shaper modification techniques to obtain robustness. Sensor feedback is used to tune the input shaper such that the residual vibration is decreased. Some of these approaches include that of Tzes and Yurkovich [26] and Khorrami, et al. [25], who used on-line adaptive schemes to update the input shaper parameters. Bodson used a recursive least-squares technique to tune the input shaper parameters [36]. Magee and Book modified the input shaper as a function of the system configuration [18].

2.4 Concurrent Design of Command Shaping and Feedback Control

Given that command shaping can greatly reduce the vibration of the system, it reduces the burden on the feedback controller. Therefore, the feedback control design becomes easier; it does not have to be concerned with reducing vibration induced by the reference command. The design of the feedback controller can be primarily based on

disturbance rejection and stability, which are its natural strengths. Given this realization, the question arises as to how to optimize the combined design of the feedback and command shaping components.

One method assumes a PD feedback controller and then concurrently chooses the PD gains and the input shaper impulses while satisfying performance specifications [56], [63]. The design method takes into account limits on allowable overshoot, residual vibration, and actuator effort. Furthermore, the structure of the method allows a wide range of performance requirements, such as disturbance rejection, to be integrated into the design. The results indicate that PD feedback control enhanced with input shaping provides better performance than PD control alone. This effect is demonstrated in Figure 10 where the settling time is shown as a function of the damping ratio of the system. With PD control alone, the minimum settling time occurs near $\zeta=0.7$ - the classic solution. However, when input shaping is used, the settling time can be greatly reduced and this occurs when the controller is tuned to have a small damping ratio.
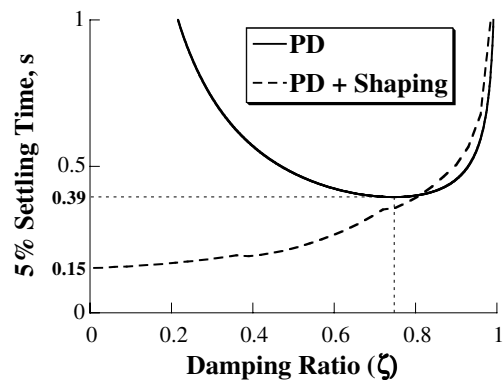
Figure 10: Settling Time vs. Damping Ratio

2.5 Shaper Design in the S-Plane and Z-Plane

The effect of command shaping is to place zeros at or near the flexible poles of the system. This idea was well documented by Bhat and Mui [10]. This realization leads to straightforward design procedures in the z-plane that were first discussed by Murphy and Watanabe [16]. Singh and Vadali [23] illustrated that a time-delay filter designed to cancel the poles of the system results in the same solu-

tion as the posicast control developed by Smith [1]. They also illustrated that cascading multiple versions of the time-delay filter resulted in the robust shaper that was proposed by Singer and Singer. Singh and Vadali also proposed a simple technique to design time-delay filters using the specified time spacing of the sampling period [32].

Seth used z-plane analysis to design a digital shaper for reducing vibration in a coordinate measuring machine [27]. Tuttle developed a simple step-by-step method to design multiple-mode input shapers in the discrete time domain by bringing together previous methods [30]. Additionally, Tuttle directly addressed the issue of time optimality for digital shapers by presenting a method for finding a positive impulse shaper that had the shortest time duration. Like Seth, Jones used z-plane analysis to design a digital shaper for reducing vibration in a coordinate measuring machine [54]. Additionally, Jones indicated the requirements on shaper duration to obtain an input shaper with only positive impulses.

Magee applied a digital shaping filter to a system with varying parameters by modifying the input shaper duration to account for system parameter variations [18]. This work verified the difficulty of changing shaper duration that was predicted by Murphy and Watanabe. More recently, Park et al. extended the z-plane based design of digital input shapers to more robust shapers [59]. In particular, Park devised a discrete time sensitivity expression. This expression was used to design very robust multiple hump input shapers directly in the z-plane [47].

3 Saturating Controllers

The problem of design of optimal control with limits on control authority has been of interest for decades. When cost functions such as maneuver time, or fuel or a weighted combination of fuel and time are considered, the resulting optimal control profiles are bang-bang or bang-off-bang implying that the controller is turned on to the extreme values or is turned off. The problem of design of time-optimal control profiles for flexible structures has been of increasing interest over the past two decades. There have been numerous computa-

tional approaches presented to deal with the effect of flexibility. Most of these deal with single input rest-to-rest problems under two classes: near-minimum time control and exact minimum-time control.

The first category is based on smooth approximations to the time-optimal control for an equivalent rigid body. This is applicable where the applied input can be smoothly varied and are not restricted to an on-off set. Junkins et al. [9] parameterize a single switch bang-bang profile using cubic polynomials in time and illustrate that the residual vibration of a flexible structure can be significantly reduced for a small penalty in maneuver time. Vadali et al. [33] used the arctan to approximate the signum function and used a parameterized smooth control profiles to determine near-time optimal control profiles for three dimensional attitude control of $ASTREX$, a flexible spacecraft testbed.

The second category studies the exact time-optimal control problem. The determination of time-optimal control profiles for flexible slewing structures with limited control authority has been addressed by Singh et al. [7]. They illustrate that the time-optimal control profile for un-damped systems is antisymmetric about the mid-maneuver time. Hablani [11] studied the same problem, but with damped modes. Ben-Asher et al. [14], present an elegant technique to prove the time-optimality of the control profiles. It is well known that the time-optimal control profile is highly sensitive to errors in system parameters. Liu and Wie [15] present a technique to "robustify" the time-optimal control by including additional switches to the control profile. Singh and Vadali [29] propose a frequency domain approach for the design of time-optimal controllers for flexible structures. The motivation behind their work is the fact that a bang-bang input can be viewed as a summation of time-delayed step commands. They pose the problem as the design of a time-delay filter designed to cancel all the poles of the system and satisfy the rigid body boundary conditions. They use the knowledge that locating multiple zeros of the time-delay filter at the estimated location of the poles of the system, results in robustness to modeling uncertainties. They illustrate their technique by designing time-optimal and robust time-

optimal control profiles for rest-to-rest and spin-up maneuvers for the benchmark floating oscillator problem.

This section will discuss the design of robust time and weighted fuel-time optimal controllers. The benchmark floating oscillator problem [21], will be used to illustrate the design technique. The design problem is posed as the design of a time-delay filter which generate the bang-bang or bang-off-bang control profile when it is driven by a step input. The knowledge that locating multiple zeros of the time-delay filter at the estimated location of the poles of the system will result in robustness to uncertainty in the location of the pole of the system will be used in the design process. For a function $f(s) = 0$, to have a minimum of two roots at $s = s_0$ requires that

$$f(s_0) = 0 \text{ and } \left.\frac{df(s)}{ds}\right|_{s_0} = 0. \qquad (15)$$

This fact is utilized to develop constraint equations to design time-delay filters with multiple zeros at specified locations.
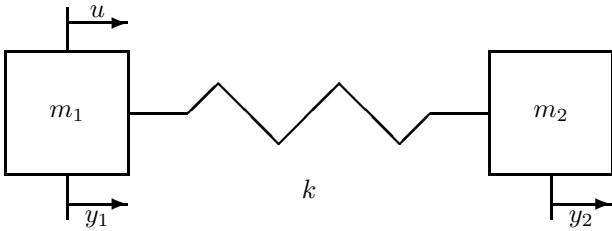

Figure 11: Floating Oscillator

The equations of motion of the benchmark floating oscillator problem illustrated in Figure 11 are

$$\begin{bmatrix} m_1 & 0 \\ 0 & m_2 \end{bmatrix} \begin{bmatrix} \ddot{y}_1 \\ \ddot{y}_2 \end{bmatrix} + \begin{bmatrix} k & -k \\ -k & k \end{bmatrix} \begin{bmatrix} y_1 \\ y_2 \end{bmatrix} = \begin{bmatrix} 1 \\ 0 \end{bmatrix} u. \qquad (16)$$

The state constraint for all the optimization problems considered in this section are

$$y_1(0) = y_2(0) = 0, \text{ and } \dot{y}_1(0) = \dot{y}_2(0) = 0$$
$$y_1(t_f) = y_2(t_f) = 1, \text{ and } \dot{y}_1(t_f) = \dot{y}_2(t_f) = 0 \quad (17)$$

and the normalized control is subject to the constraint

$$-1 \leq u \leq 1. \qquad (18)$$

The nominal values of the parameters of the system are

$$m_1 = m_2 = k = 1 \qquad (19)$$

The equations of motion can be decoupled by the similarity transformation

$$\theta = \frac{1}{2}(y_1 + y_2) \text{ and } q = \frac{1}{2}(y_2 - y_1) \qquad (20)$$

resulting in the equations of motion

$$\ddot{\theta} = \frac{1}{2}u$$

$$\ddot{q} + 2q = -\frac{1}{2}u, \qquad (21)$$

and the corresponding boundary conditions are

$$\theta(0) = q(0) = 0 \text{ and } \dot{\theta}(0) = \dot{q}(0) = 0$$
$$\theta(t_f) = 1, q(t_f) = 0 \text{ and } \dot{\theta}(tf) = \dot{q}(t_f) = 0. \quad (22)$$

The decoupled equations are used to derive the constraint equations for the optimization problem since this approach can be generalized for any number of modes.
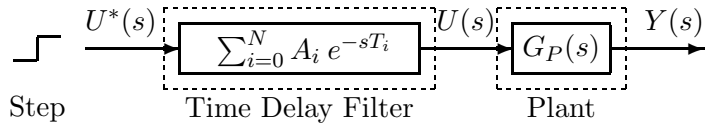

Figure 12: Time Delay Filter Structure

In this paper, the design of control profiles subject to the aforementioned control constraint is posed as the design of a time-delay filter. The output of this time-delay filter subject to a step input is the optimal switching control profile, as shown in Figure 12. For instance to generate a single switch bang-bang control profile which is the time-optimal control profile for a rigid body system, the transfer function of the time-delay filter is

$$G(s) = 1 - 2exp(-sT) + exp(-2sT), \qquad (23)$$

and the optimal control profile is given by the equation

$$u(s) = \frac{1}{s}(1 - 2exp(-sT) + exp(-2sT)). \qquad (24)$$

The generic transfer function of a time-delay filter is represented as

$$G(s) = \sum_{i=0}^{N} A_i exp(-sT_i), \text{ where } T_0 = 0, \qquad (25)$$

and where A_i belongs to the set

$$A_i = \begin{bmatrix} -2 & -1 & 1 & 2 \end{bmatrix} \qquad (26)$$

to guarantee that the output of the time-delay filter is either bang-bang or bang-off-bang. For rest-to-rest maneuver of flexible structures, the constraint which guarantees zero residual vibration is derived by requiring a set of zeros of the time-delay filter to cancel the under-damped poles of the system. For a system with a set of under-damped poles at

$$s = \sigma \pm j\omega, \qquad (27)$$

the constraint equations are

$$\sum_{i=0}^{N} A_i exp(-\sigma T_i)cos(\omega T_i) = 0, \qquad (28)$$

and

$$\sum_{i=0}^{N} A_i exp(-\sigma T_i)sin(\omega T_i) = 0, \qquad (29)$$

which are derived by forcing the real and imaginary parts of the transfer function of the time-delay filter to zero at $s = \sigma \pm j\omega$. Note, that this is equivalent to the conditions given in Equations 2.

To satisfy the boundary conditions for the rigid body for the rest-to-rest maneuver, the transfer function of the time-delay filter should have two zeros at the origin of the complex plane to cancel the rigid body poles, resulting in the constraint equation

$$\sum_{i=0}^{N} A_i = 0 \qquad (30)$$

and

$$\sum_{i=0}^{N} A_i T_i = 0 \qquad (31)$$

The constraint to satisfy the total rigid body displacement is

$$\theta(t_f = T_N) = \frac{1}{2} \sum_{i=0}^{N} A_i \frac{(T_N - T_i)^2}{2}. \qquad (32)$$

Finally, to desensitize the control profile to uncertainties in the location of the under-damped poles of the system, constraints are derived which place multiple zeros of the time-delay filter at the estimated location of the poles of the system. These

constraints are

$$\sum_{i=0}^{N} A_i T_i exp(-\sigma T_i)cos(\omega T_i) = 0, \qquad (33)$$

and

$$\sum_{i=0}^{N} A_i T_i exp(-\sigma T_i)sin(\omega T_i) = 0 \qquad (34)$$

which are equivalent to the zero derivative constraint given in Equation 13.

Since the constraints are nonlinear, there are potentially numerous parameter sets which satisfy all of the constraints. The sufficient conditions for the optimality of the control profile are dependent on the cost function to be optimized for and a general approach to verify the optimality is not available. For un-damped system, it has been shown that the control profile is anti-symmetric about the mid-maneuver time. This fact can be exploited to reduce the number of parameters to be optimized for.

3.1 Time-Optimal Control

The time-optimal control profile for the un-damped benchmark problem can be determined by solving the following parameter optimization problem which is derived by exploiting the anti-symmetric properties of the control profile (Figure 13):

$$\min J = T_2^2 \qquad (35)$$

$$-2cos(\omega(T_2 - T_1)) + 1 + cos(\omega T_2) = 0 \qquad (36)$$

$$\frac{1}{2}(2T_2^2 - (2T_2 - T_1)^2 + T_2^2 - T_1^2) = 1, \qquad (37)$$

where

$$T_0 = 0, \, T_1 = T_1, \, T_2 = T_2, \, T_3 = 2T_2 - T_1, \, T_4 = 2T_2$$

$$A_0 = 1, \, A_1 = -2, \, A_2 = 2, \, A_3 = -2, \, A_4 = 1. \quad (38)$$

To desensitize the controller to the frequency of the flexible mode, two switches are added to the control profile and the problem is

$$\min J = T_3^2 \qquad (39)$$

$$-2cos(\omega T_{31}) + 2cos(\omega T_{32}) + 1 + cos(\omega T_3) = 0 \qquad (40)$$

$$-2T_{31}sin(\omega T_{31}) + 2T_{32}sin(\omega T_{32}) + T_3 sin(\omega T_3) = 0 \qquad (41)$$

$$2T_3^2 - (2T_3 - T_1)^2 + (2T_3 - T_2)^2 - T_3^2 + T_2^2 - T_1^2 = 2. \qquad (42)$$

where the double subscript represent $P_{ij} = P_i - P_j$. Having solved for the switch times, their optimality have to be verified. This is achieved by solving
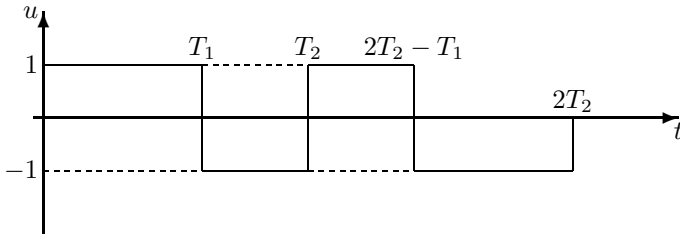
Figure 13: Antisymmetric Control Profile

for the costates and the resulting switching curve is used to corroborate the optimality of the solution. Details of these techniques have been presented in [7], [15], [14], [29] etc.

Figure 14 illustrates the time-optimal control profile and the robust control profile and the corresponding energy sensitivity curves. It is clear that local to the nominal spring stiffness there is a significant improvement of the insensitivity of the robust control profile.
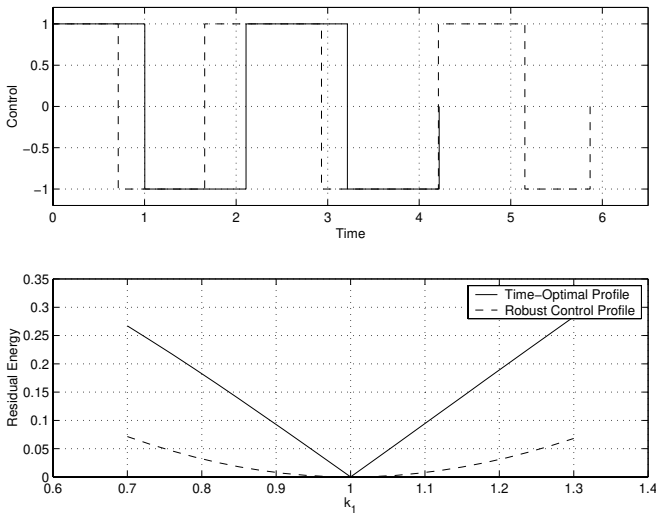

Figure 14: Control and Residual Energy Variation

The variation of the structure of time-optimal control profiles as a function of damping has been illustrated by Pao [37] and Singh [35]. For a two-mass system connected by a spring and a damper, the control profile changes from a three switch for un-damped systems to a five switch and back to a three switch control profile, as the damping is increased. Time-optimal control profile for mult-mode systems have been derived in [45]. Tuttle and Seering, developed a Matlab toolbox to gen-

erate time-optimal commands for a wide range of flexible systems [55].

3.2 Fuel/Time Optimal Control

The Fuel/Time optimal control profile for the benchmark problem can be represented as shown in Figure 15 where the anti-symmetric property for undamped systems is exploited.
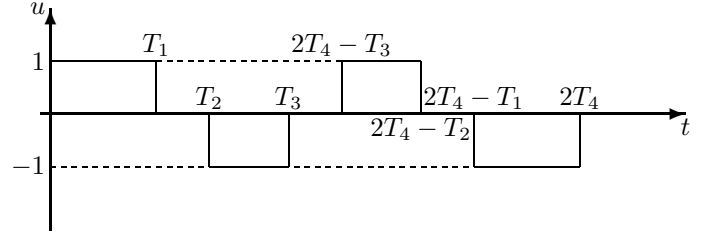

Figure 15: Fuel-Time Optimal Control Profile

Minimizing the cost function

$$J = \int_0^{t_f} (1 + \alpha|u|)\, dt \qquad (43)$$

where the cost function J is a weighted $(\alpha > 0)$ combination of the maneuver time and fuel consumed results in the parameter optimization problem:

$$\min J = 2T_4 + 2\alpha\,[T_{43} + T_{21}] \qquad (44)$$

$$cos(\omega T_{43}) - cos(\omega T_{42}) - cos(\omega T_{41}) + cos(\omega T_4) = 0 \qquad (45)$$

$$\frac{1}{2}(-T_1^2 - T_2^2 + T_3^2 + 2T_4(T_1 + T_2 - T_3)) = 1. \qquad (46)$$

Solving for the optimal control profile as a function of α, the control profile changes from a three switch bang-bang profile for $\alpha = 0$, to a six switch bang-off-bang control profile which simplifies to a two switch bang-bang profile for $\alpha > 0.6824$, for the benchmark problem, as shown in Figure 16.

Hartmann and Singh [50] present a general development of the necessary and sufficient conditions for optimality of the fuel/time optimal control profiles for system of order higher than the benchmark problem.

3.3 Minimax Control

The techniques to desensitize the controller to modeling errors which have been presented to this point, only require information about the nominal values of the model parameters. The resulting controllers are robust in the vicinity of the nominal parameters of the system. However, in
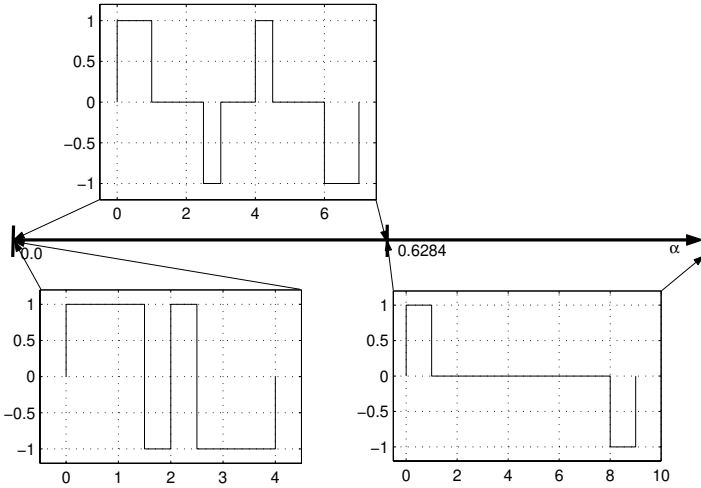
Figure 16: Spectrum of Fuel/Time Optimal Control

numerous applications, the range of uncertainty is know and often the distribution of the uncertainty is know. There is thus a desire to formulate optimization problems which includes the information about the range of uncertainty, in the design of controllers. The technique expounded in this section is germane to the design of the input shapers, as well as for the design of saturating controllers.

For a mechanical system undergoing rest-to-rest maneuvers, the model can be represented as

$$M\ddot{y} + C(p)\dot{y} + K(p)y = Dr \qquad (47)$$

where M is a positive definite mass matrix, and K and C, the stiffness and damping matrices. K is positive semi-definite when the model of the system includes rigid body modes and is positive definite otherwise. p is a vector of uncertain parameters whose elements satisfy the constraints:

$$p_i^{lb} \leq p_i \leq p_i^{ub} \qquad (48)$$

where p_i^{lb} and p_i^{ub} represent the lower and upper bounds on the parameters respectively. The goal here is to design a saturating controller with the objective of minimizing the maximum value of the residual energy

$$\min_x \max_p F$$

$$F = \frac{1}{2}\dot{y}^T M\dot{y} + \frac{1}{2}(y-y_f)^T K(y-y_f) + \frac{1}{2}(y_r-y_{rf})^2 \qquad (50)$$

where x is a vector of parameters which define the saturating controller and y_f corresponds to the

final displacement states of the system. The above equation will be referred to as the pseudo-energy function since it is associated with a hypothetical spring whose potential energy is zero when $y = y_f$. The pseudo-energy function is evaluated at the final time, i.e., the end of the maneuver. The last term is added to guarantee that the cost function is positive definite.

Minimax bang-bang controllers are designed for the floating oscillator benchmark problem to illustrate the proposed technique. The time-optimal control of the benchmark problem is a 3-switch anti-symmetric bang-bang control profile. The thin solid line in Figure 17 illustrates the variation of the residual energy of the time-optimal control to variations in the spring stiffness. A 3-switch minimax controllers is designed without the constraint that the residual energy be zero at the nominal value of the spring stiffness. The thin dashed line illustrates that the maximum magnitude of the residual energy over the uncertain range ($0.7 < k < 1.3$) has been minimized, but at the cost of non-zero residual energy for the nominal model. Next, the 5-switch robust time-optimal control profile is designed to force the slope of the sensitivity curve for the nominal system to go to zero. The think solid line illustrate the significant reduction of the residual energy over the entire uncertain range. However, this is achieved at a cost of increased maneuver time. Finally, a 5-switch minimax controller is designed and the thick dashed line illustrates the improvement over the robust 5-switch time-optimal controller. The resulting sensitivity curve is similar to the curve for extra-insensitivity input shapers [40].

3.4 Finite Jerk Time-Optimal Control
Recently, Muenchhof and Singh [58] and Lim et al. [53] have proposed a optimal control formulation which includes limits on the rate of change of control (Jerk). The control rate profiles are bang-bang or bang-off-bang as a function of the permitted jerk and the maneuver distance, for a rest-to-rest maneuver. The problem in [58], is posed as the design of time-delay filter which is parameterized to generate a bang-bang or bang-off-bang profile whose integral is the control input to the plant. Figure 18 illustrates the variation of the switches and change of the structure of the control profile as a function of permitted jerk for the
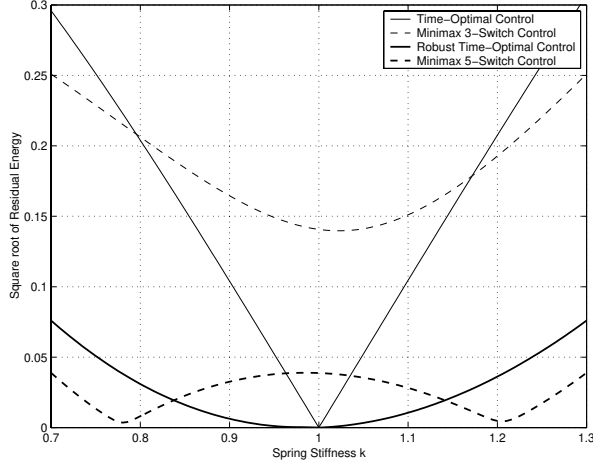
Figure 17: Residual Energy Distribution

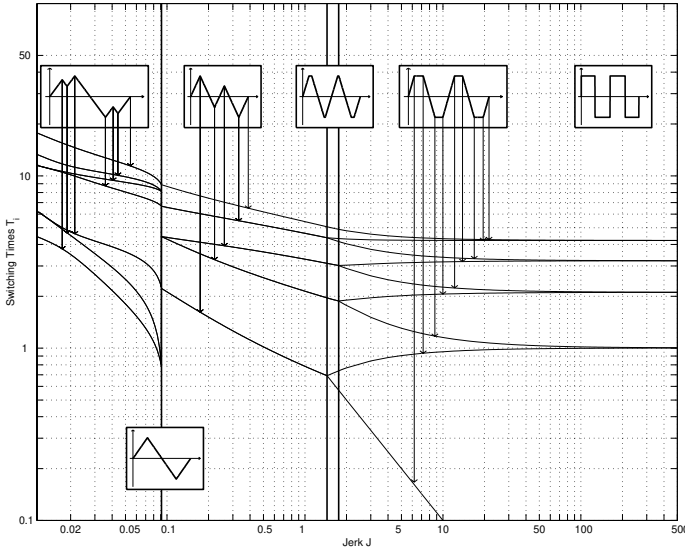benchmark floating oscillator problem.

Figure 18: Switch Time Trajectories

It can be seen that the structure of the control profile changes significantly. The thick vertical lines indicate the value of jerk where switches collapse or are spawned. It is interesting to note that the maneuver time only increases marginally. as the permitted jerk is decreased from ∞ to 2.

4 Nonlinear Systems

The technique presented for the design of controller which are robust to modeling uncertainties included location of multiple zeros of the time-delay filter at the estimated location of the poles of the system. This approach obviously cannot be used for the design of robust control profiles for nonlinear systems. Liu and Singh [41] proposed a technique where the sensitivity state equations are included in the problem formulation with the constraint that the sensitivity states be forced to zero at the final time. For the nonlinear system

$$\underline{\dot{x}} = \underline{f}(\underline{x}, u, \underline{p}), \tag{51}$$

where $\underline{p}$ is the vector of uncertain parameters, the sensitivity state equations are

$$\frac{d\underline{\dot{x}}}{dp_i} = \frac{\partial \underline{f}}{\partial p_i} + \sum_{j=1}^{n} \frac{\partial \underline{f}}{\partial x_j} \frac{dx_j}{dp_i}. \tag{52}$$

The control profile should in addition to satisfying the boundary conditions of the system states x, must also force

$$\left. \frac{d\underline{x}}{dp_i} \right|_{t_f} = 0, \ \forall p_i. \tag{53}$$

To illustrate this approach, consider the benchmark problem with a nonlinear spring whose model is

$$m_1\ddot{y}_1 + k_1(y_1 - y_2) + k_2(y_1 - y_2)^3 = u \tag{54}$$
$$m_2\ddot{y}_2 - k_1(y_1 - y_2) - k_2(y_1 - y_2)^3 = 0. \tag{55}$$

The sensitivity state equations are

$$m_1\frac{d\ddot{y}_1}{dk_1} + y_{12} + k_1\frac{dy_{12}}{dk_1} + 3k_2y_{12}^2\frac{dy_{12}}{dk_1} = 0 \tag{56}$$

$$m_2\frac{d\ddot{y}_2}{dk_1} - y_{12} - k_1\frac{dy_{12}}{dk_1} - 3k_2y_{12}^2\frac{dy_{12}}{dk_1} = 0 \tag{57}$$

$$m_1\frac{d\ddot{y}_1}{dk_2} + k_1\frac{dy_{12}}{dk_2} + y_{12}^3 + 3k_2y_{12}^2\frac{dy_{12}}{dk_2} = 0 \tag{58}$$

$$m_2\frac{d\ddot{y}_2}{dk_2} - k_1\frac{dy_{12}}{dk_2} - y_{12}^3 - 3k_2y_{12}^2\frac{dy_{12}}{dk_2} = 0 \tag{59}$$

The time-optimal control profile is designed to satisfy the boundary conditions

$$y_1 = y_2 = \dot{y}_1 = \dot{y}_2 = \frac{dy_1}{dk_1} = \frac{d\dot{y}_1}{dk_1} = \frac{dy_1}{dk_2} = \frac{d\dot{y}_1}{dk_2} = 0 \bigg|_{t=0}$$

$$y_1 = y_2 = 1, \dot{y}_1 = \dot{y}_2 = \frac{dy_1}{dk_1} = \frac{d\dot{y}_1}{dk_1} = \frac{dy_1}{dk_2} = \frac{d\dot{y}_1}{dk_2} = 0 \bigg|_{t=t_f}.$$
$$\tag{60}$$

Figure 19 illustrates the reduction in residual vibration of the desensitized time-optimal control, compared to the time-optimal control in the vicinity of the nominal values of the spring coefficients. The maneuver time of the two time-optimal control profile is $t_f = 4.1514$, and for the desensitized control profile is $t_f = 6.2439$. It is clear the insensitivity to model parameters is achieved at a cost of increased maneuver time.
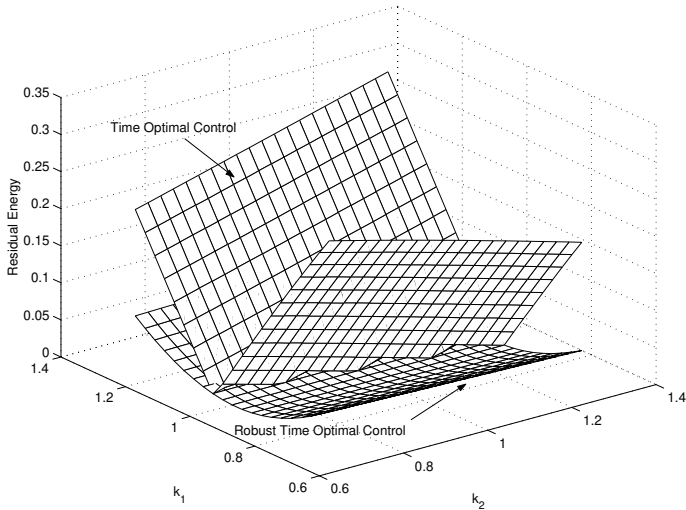
Figure 19: Sensitivity Plot for the 3/9 switch Control

5 Applications

Given the simple approach and ease of implementation of basic input shaping techniques, they have been used in a variety of applications. The wide spread use is also attributable to the robustness that can be added to many of the techniques. One major area of success has been on cranes and crane-like structures. Starr wrote an early paper that implemented a ZV-like shaping scheme on a crane [6]. Groups at Sandia and Oak Ridge National labs have been especially active in this area [28], [20], [43]. Their approach has been similar to the input shaping described in Section 2; however, the shaping filter utilized has often been an IIR filter instead of a FIR filter. Their technique has also been utilized to control sloshing fluids [43]. Another approach, which has been implemented on some large gantry cranes, designed input shapers to suppress vibration over the expected operating ranges of the cranes [44]. Figure 20 shows the reduction in residual vibration as a function of the hoist cable length.
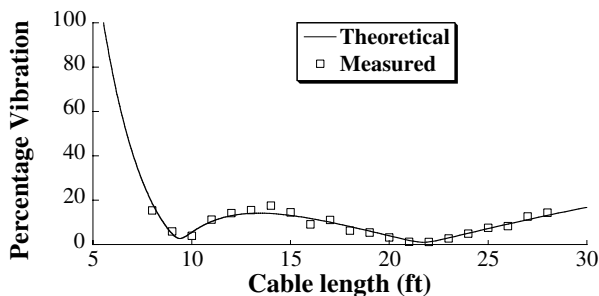

Figure 20: Vibration Reduction vs. Cable Length

High tech manufacturing is perhaps the area with the highest number of input shaping applications. Shaping was an important component of a control system developed for a wafer stepper [48]. Multiple modes of a silicon-handling robot were eliminated with input shaping [31]. Accuracy of coordinate measuring machines has been improved with command shaping [54], [27], [39]. The throughput of a hard-disk-drive-head testing machine was significantly improved with shaping [46]. Figure 21 shows the position response of the reading heads during testing both before and after input shaping was implemented. The greatly reduced settling time allowed for much higher throughput. Command shaping has been combined with vision sensing and learning control on x-y-z gantry-type automation machinery [62]. Figure 22 shows the decrease in tip vibration of the machine as the learning controller adapts the input shaper to the system vibration during repeated motion.
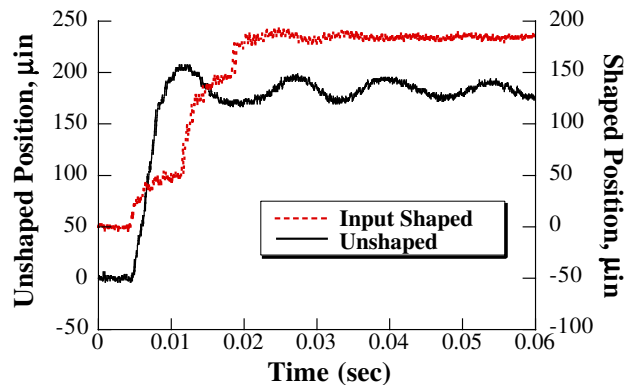

Figure 21: Head Response During Testing

Applications involving shaping the commands to on-off actuators or saturating actuators are fewer than with real-time shaping, but there have still been a number of successes. In fact, the crane control scheme whose results are shown in Figure 20 uses an on-off actuator switching algorithm to accomplish the vibration reduction. Recently, a technique for shaping the momentum dumping of spacecraft was adopted as a baseline design for the next generation space telescope [60].

References

[1]   Smith, O. J. M., "Posicast Control of Damped Oscillatory Systems", Proc. of the IRE, 1957, pp 1249-1255.

[2]   Calvert, J. F. and Gimpel, D. J., "Method and Apparatus for Control of System Output Response to System Input", U.S. Patent #2,801,351, 1957.
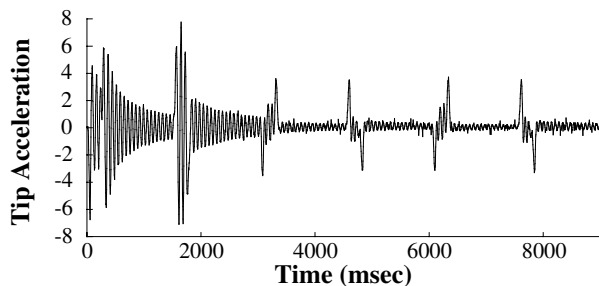
Figure 22: Adaptive Command Shaping

[3]   Tallman, G. H., Smith, O. J. M., 1958, "Analog Study of Posicast Control", IRE Transactions on Automatic Control, Vol. 3, pp 14-21.

[4]   Farrenkopf, R. L., 1979, "Optimal Open-Loop Maneuver Profiles for Flexible Spacecraft", *J. of Guidance, and Control*, Vol. 2, No. 6, pp 491-498

[5]   Swigert, C. J., "Shaped Torques Techniques", J. of Guidance and Control, Vol. 3, 1980, pp 460-467.

[6]   Starr, G. P., "Swing-Free Transport of Suspended Objects With a Path-Controlled Robot Manipulator", *J. of Dynamic Systems, Measurement and Control*, vol. 107, pp. 97-100, 1985.

[7]   Singh, G., Kabamba, P. T., McClamroch, N. H., 1989, "Planar, Time-Optimal, Rest-to-Rest Slewing Maneuvers of Flexible Spacecraft", *J. of Guidance, Control, and Dynamics*, Vol. 12, No. 1, pp 71-81.

[8]   Singer, N. C., and Seering, W. P., "Preshaping Command Inputs to Reduce System Vibrations", *ASME J. of Dynamic Systems, Measurement and Control*, Vol. 112, 1990, pp 76-82.

[9]   Junkins, J., L., Rahman, Z., Bang, H., 1990, "Near-Minimum Time Maneuvers of Flexible Vehicles: A Liapunov Control Law Design Method", *Mechanics and Control of Large Flexible Structures*, Published by the American Institute of Aeronautics and Astronautics, Inc., Washington.

[10]   Bhat, S. P. and Miu, D. K., 1990, "Precise Point-to-Point Positioning Control of Flexible Structures", *J. of Dynamic Sys., Meas., and Control*, Vol. 112(4), pp. 667-674

[11]   Hablani, B. H., 1990, "Zero-Residual-Energy, Single-Axis Slew of Flexible Spacecraft with Damping, Using Thrusters: A Dynamic Approach". *Proc. of the 1990 AIAA Guidance, Navigation, and Control Conference,*

[12]   Singhose, William E., Singer, Neil C., Seering, Warren P.,1990, "Shaping Inputs to Reduce Vibration: A Vector Diagram Approach" *Proc. of the 1990 IEEE International Conference of Robotics and Automation,* Vol. 2, Cincinnati, Ohio, pp. 922-927.

[13]   Hyde, J. M., Seering, W. P., 1991, "Multiple Mode Vibration Suppression in Controlled Flexible Systems" *MIT Space Engineering Research Center report, SERC #3-91*

[14]   Ben-Asher, J., Burns, J. A. and Cliff, E. M., 1992, "Time-Optimal Slewing of Flexible Spacecraft", *J. of Guidance, Control, and Dynamics*, Vol. 15(2), pp. 360-367.

[15]   Liu, Q. and Wie, B., 1992, "Robust Time-Optimal Control of Uncertain Flexible Spacecraft", *J. of Guidance, Control, and Dynamics*, Vol. 15(3), pp. 597-604

[16]   Murphy, B. R. and Watanabe, I., 1992 "Digital Shaping Filters for Reducing Machine Vibration", *IEEE Transactions on Robotics and Automation*, Vol. 8(April), pp. 285-289.

[17]   Singer, N. C. and Seering, W. P., "An Extension of Command Shaping Methods for Controlling Residual Vibration Using Frequency Sampling", *IEEE International Conference on Robotics and Automation*, Nice, France, 1992.

[18]   Magee, D. and Book, W., "The Application of Input Shaping to a System with Varying Parameters", *Japan/USA Symposium on Flexible Automation*, 1992.

[19]   Singer, N. C. and Seering, W. P., "An Extension of Command Shaping Methods for Controlling Residual Vibration Using Frequency Sampling", *IEEE International Conference on Robotics and Automation*, Nice, France, 1992.

[20]   Noakes, M. W. and Jansen, J. F., "Generalized Inputs for Damped-Vibration Control of Suspended Payloads", *Robotics and Autonomous Systems*, vol. 10, pp. 199-205, 1992.

[21]   Wie, B. and Bernstein, D., "Benchmark Problems for Robust Control Design", *J. of Guidance, Control and Dynamics*, Vol. 15, No. 5, 1992, pp 1057-1058.

[22]   Singh, T. and Vadali, S. R., 1993, "Input-Shaped Control of Three-Dimensional Maneuvers of Flexible Spacecraft", *J. of Guidance, Control, and Dynamics*, Vol. 16(6), pp. 1061-1068.

[23]   Singh, T. and Vadali, S. R., 1993, "Robust Time-Delay Control", *ASME J. of Dynamic Systems, Measurement, and Control*, Vol. 115, pp. 303-306.

[24]   Singh, T., Heppler, G. R., 1993, "Shaped Input for Multimode System" *ASME J. of Dynamic Systems, Measurement and Control*, Vol. 115, 1993, pp 341-347.

[25]   Khorrami, F., Jain, S., and Tzes, A., "Adaptive Nonlinear Control and Input Preshaping for Flexible-Link Manipulators", *American Control Conf.*, San Francisco, CA, 1993.

[26]   Tzes, A., and Yurkovich, S., "An Adaptive Input Shaping Control Scheme for Vibration Suppression in Slewing Flexible Structures", *IEEE Transactions on Control Systems Technology*, Vol. 1, pp. 114-121, 1993.

[27]   Seth, N., Rattan, K. and Brandstetter, R., "Vibration Control of a Coordinate Measuring Machine", *IEEE Conf. on Control Apps.*, Dayton, OH, 1993.

[28]   Feddema, J. T., "Digital Filter Control of Remotely Operated Flexible Robotic Structures", *American Control Conf.*, San Francisco, CA, 1993.

[29]   Singh, T. and Vadali, S. R., "Robust Time-Optimal Control: Frequency Domain Approach", *AIAA J. of Guidance, Control and Dynamics*, Vol. 17, No. 2, 1994, pp 346-353.

[30]   Tuttle, T. D. and Seering, W. P., "A Zero-placement Technique for Designing Shaped Inputs to Suppress Multiple-mode Vibration", *American Control Conf.*, Baltimore, MD, 1994.

[31]   Rappole, B. W., Singer, N. C., and Seering, W. P., "Multiple-Mode Impulse Shaping Sequences for Reducing Residual Vibrations", *23rd Biennial Mechanisms Conference*, Minneapolis, MN, 1994.

[32] Singh, T., Vadali, S. R., 1995, "Robust Time-Delay Control of Multimode Systems", International J. of Control, Vol. 62, No. 6, pp 1319-1339.

[33] Vadali, S. R., Carter, M. T., Singh, T., and Abhyankar, N. S., 1995,"Near-Minimum-Time Maneuvers of Large Structures: Theory and Experiment", *J. of Guidance, Control and Dynamics*, Vol. 18, No. 6, pp 1380-1385.

[34] Singh, T., 1995, "Fuel/Time Optimal Control of the Benchmark Problem", *J. of Guidance, Control, and Dynamics*, Vol. 18(6), pp. 1225-31.

[35] Singh, T., 1996, "Effect of Damping On the Structure of Time-Optimal Controllers", *J. of Guidance, Control and Dynamics*, Vol.19, No. 5, pp 1182-1184.

[36] Bodson, M., "Experimental Comparison of Two Input Shaping Methods for the Control of Resonant Systems", *IFAC World Congress*, San Francisco, CA, 1996.

[37] Pao. L. Y., "Minimum-Time Control Characteristics of Flexible Structures", *J. Guidance, Control, and Dynamics*, 19(1): 123-129, Jan.-Feb. 1996.

[38] Singhose, W. E., Seering, W. P. and Singer, N. C., "Input Shaping for Vibration Reduction with Specified Insensitivity to Modeling Errors", *Japan-USA Sym. on Flexible Automation*, Boston, MA, 1996.

[39] Singhose, W., Singer, N., and Seering, W., "Improving Repeatability of Coordinate Measuring Machines with Shaped Command Signals", *Precision Engineering*, Vol. 18, pp. 138-146, 1996.

[40] Singhose, W., Derezinski, S. and Singer, N., "Extra-Insensitive Input Shapers for Controlling Flexible Spacecraft", *AIAA J. of Guidance, Control, and Dynamics*, vol. 19, pp. 385-91, 1996.

[41] Liu, S-W., and Singh, T., 1997, "Robust Time-Optimal Control of Nonlinear Structures with Parameter Uncertainties", *ASME J. of Dynamic Systems, Measurement and Control*, Vol. 119, No. 4, 1997, pp 743-748.

[42] Singhose, W., Banerjee, A. and Seering, W., 1997, "Slewing Flexible Spacecraft with Deflection-Limiting Input Shaping", *J. of Guidance, Control, and Dynamics*, Vol. 20(2), pp. 291-298.

[43] Feddema, J., Dohrmann, C. , Parker, G., Robinett, R., Romero, V. and Schmitt, D., "Control for Slosh-Free Motion of an Open Container", *IEEE Control Systems*, vol. 17, pp. 29-36, 1997.

[44] Singer, N., Singhose, W., and Kriikku, E., "An Input Shaping Controller Enabling Cranes to Move Without Sway", *ANS 7th Topical Meeting on Robotics and Remote Systems*, Augusta, GA, 1997.

[45] Singhose, W., Pao, L. Y., and Seering, W. P., "Slewing Multi-Mode Flexible Spacecraft Using Zero Derivative Robustness Constraints", *J. of Guidance, Control and Dynamics*, Vol. 20, 1997, pp 204-206.

[46] Singhose, W., Singer, N., and Seering, W., "Time-Optimal Negative Input Shapers", *J. of Dynamic Systems, Measurement, and Control*, vol. 119, pp. 198-205, 1997.

[47] W. E. Singhose, L. J. Porter, T. D. Tuttle, and N. C. Singer, "Vibration Reduction Using Multi-Hump Input Shapers", *J. of Dynamic Systems, Measurement, and Control*, vol. 119, pp. 320-326, 1997.

[48] deRoover, D., Sperling, F. B. and Bosgra, O. H., "Point-to-Point Control of a MIMO Servomechanism", *American Control Conference*, Philadelphia, PA, 1998.

[49] Pao, L. Y. and Singhose, W. E., "Robust Minimum Time Control of Flexible Structures", *Automatica*, 34(2): 229-236, Feb. 1998.

[50] Hartmann, R., and Singh, T., "Fuel/Time Optimal Control of Flexible Structures: A Frequency Domain Approach', *Journal of Vibration and Control*, Sept., 1999, Vol. 5, No. 5, pp 795-817.

[51] Singhose, W., Singh, T., Seering W., 1999, "On-Off Control with Specified Fuel Usage", *ASME J. of Dynamic Systems, Measurement and Control*, Vol. 121(2), pp 206-212.

[52] Pao, L. and Lau, M. A., "The Expected Residual Vibration of Traditional and Hybrid Input Shaping Designs", *J. Guid., Contr., & Dyn.*, vol. 22, pp. 162-165, 1999.

[53] Sungyung Lim, Homer D. Stevens, and Jonathan P. How "Input Shaping Design for Multi-Input Flexible Systems", *ASME J. of Dynamic Systems, Measurement and Control*, Vol. 121(3), pp 443-447.

[54] Jones, S. and Ulsoy, A. G., "An Approach to Control Input Shaping with Application to Coordinate Measuring Machines", *J. of Dynamics, Measurement, and Control*, Vol. 121, pp. 242-247, 1999.

[55] Tuttle, and Seering, W. P. "Creating Time-Optimal Commands with Practical Constraints", *J. Guid., Contr., & Dyn.*, Vol. 22, No. 2, 1999, pp. 241-250.

[56] Kenison, M. and Singhose, W. ,"Concurrent Design of Input Shaping and Feedback Control for Insensitivity to Parameter Variations", *Sixth Int. Workshop on Advanced Motion Control*, Nagoya, Japan, 2000.

[57] Hindle, T., Singh, T., 2001, "Robust Minimum Power/Jerk control of Maneuvering Structures", *J. of Guidance, Control and Dynamics*, Vol. 24, No. 4, pp 816-826.

[58] Muenchhof, M., Singh, T., 2001, "Jerk Limited Time Optimal Control of Structures", *Proc. of the 2001 ASME International Mechanical Engineering Congress and Exposition*

[59] Park, U. H., Lee, J. W., Lin, B. D. and Sung, Y. G., "Design and Sensitivity Analysis of an Input Shaping Filter in the z-Plane", *J. of Sound and Vibration*, vol. 243, pp. 157-171, 2001.

[60] Banerjee, A., Pedreiro, N., and Singhose, W., "Vibration Reduction for Flexible Spacecraft Following Momentum Dumping with/without Slewing", *AIAA J. of Guidance, Control, and Dynamics*, Vol. 24, 2001.

[61] Lau, M. A. and Pao, L. Y., "Comparison of Input Shaping and Time-Optimal Control of Flexible Structures", *Proc. American Control Conf.*, Arlington, VA, pp. 1485-1490, June 2001.

[62] Rhim, S. and W. J. Book, "Noise Effect on Time-domain Adaptive Command Shaping Methods for Flexible Manipulator Control", *IEEE Transactions of Control Systems Technology*, Vol. 9, No. 1, 2001, pp. 84 - 92.

[63] Kenison, M. and Singhose, W., "Concurrent Design of Input Shaping and Proportional Plus Derivative Feedback Control", Accepted to the *ASME J. of Dynamic Systems, Measurement, and Control*.

Optimal
Reference Shaping
for Dynamical Systems

Theory and Applications

Tarunraj Singh
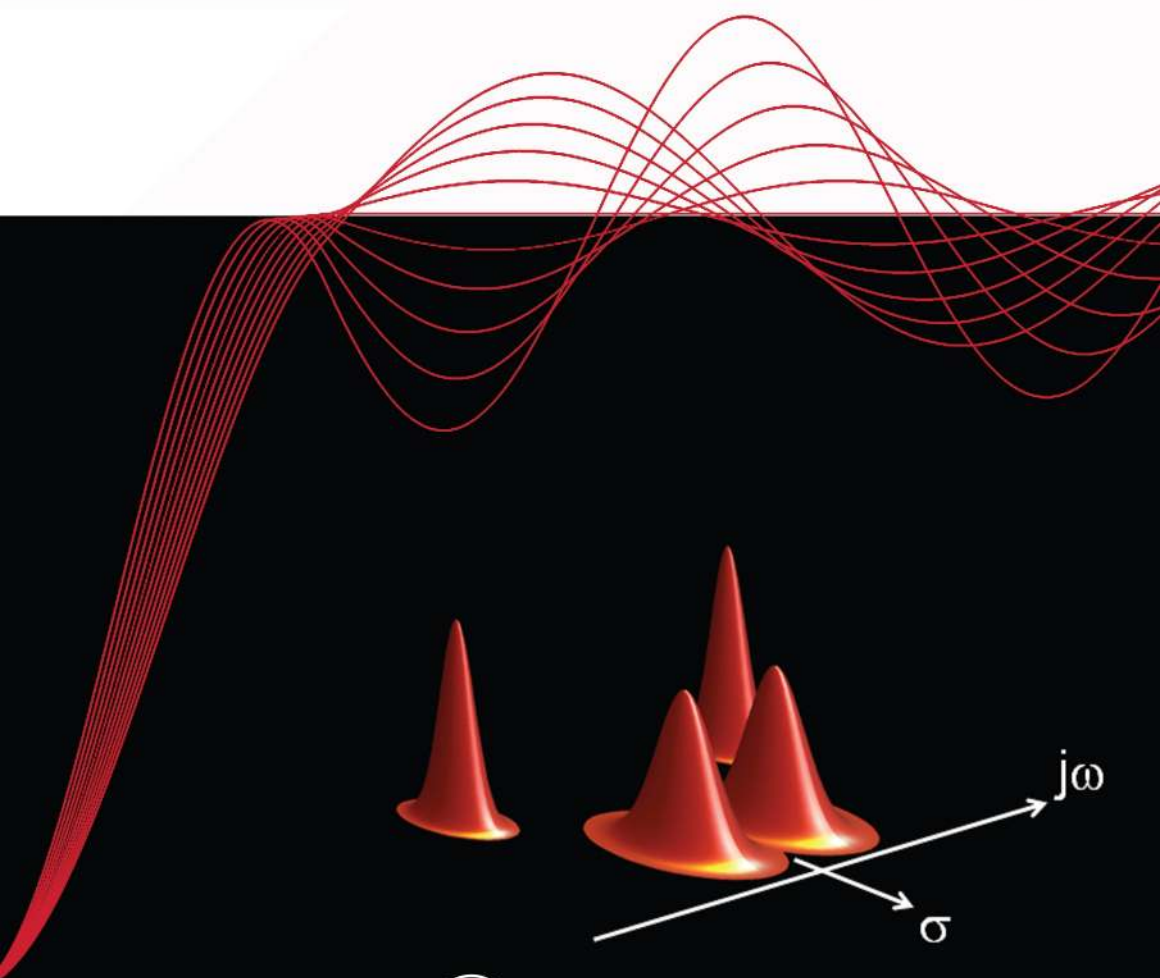
CRC Press
Taylor & Francis Group

A CHAPMAN & HALL BOOK